Design and Implementation of Density Sensor for Liquids Using Fiber Bragg Grating Sensor

Venkata Satya Chidambara Swamy Vaddadi, *Member, IEEE*, Saidi Reddy Parne, *Member, IEEE*, Vijeesh V. P., Suman Gandi, and Linga Reddy Cenkeramaddi, *Senior Member, IEEE*

***Abstract*—In this paper, an optical fiber sensor based density sensor is proposed and demonstrated experimentally. The sensor is formed by fiber Bragg grating (FBG) sensor. The proposed sensor design is very simple and versatile for density measurements of liquids. The FBG strain sensor has one end mounted to a 3D printed rigid support, and the other end connected to a 3D manufactured clamp in this sensor design. A metal ball is suspended from this clamp by a non-stretchable cord. When it is completely immersed in liquid, the liquid buoyancy force acts on it. As a result, the strain in FBG varies depending on the force applied to the ball. This results in a wavelength shift in the FBG sensor. The proposed sensor design is tested for four distinct liquids, including water, gasoline, engine oil, and acetone, and the measured density values for each were tabulated. We estimated the density of water by varying the temperature and adding salt. Based on the measurements, the sensitivity of the sensor is 2.584 pm/Kg/m^3 when the temperature of liquid changes and 3.375×10^{-2} pm/Kg/m^3 when density varied by adding salt to the liquid is reported.**

***Index Terms*—Density, fiber Bragg grating (FBG), 3D printing, oil, hotplate, density of water.**

I. Introduction

DENSITY is one of the most prevalent physical properties used to classify and characterize the fluids in the environmental, petroleum, cosmetics, food and beverages, and pharmaceuticals. Numerous products generated from petroleum are used in our everyday lives, including various oils, fuels, and petrochemicals. All the materials are a mixture of several carbon hydroxides, which need to be characterised by their physical properties, including density. To measure the density of liquids, scientists have used different ways. In nuclear liquid density measurements, they have used a nuclear gauge, which works on the simple principle of gamma-ray attenuation [1]. These gauges will require a source and detector for the measurement, also this technology requires highly sophisticated software. In the conventional way of density measurement, an oscillating U tube method is used. In this measurement, density measuring liquid needs to fill the U-shaped tube, and this tube will oscillate according to the given driving frequency [2]. Buoyancy-based approaches work great in different applications [3]–[5], including liquid level density related to the temperature and composition [6]. Online density measurement is greatly important for quality testing in storage fuel and chemicals, besides in industry where volume is regarded as metrology (ex: gasoline station) [7], [8]. This type of measurement is called indirect measurement. While in the case of direct measurement, evanescent wave coupling between the level measurement fiber/wave guide and the measured surrounding liquid. The density, viscosity, and surface tension of a liquid are important parameters for process design and coating thickness control in the paint industries. Since it releases the SO_2, NO_x, CO, non-methane volatile organic compounds (NMVOCs), they have developed a new type of viscometer to measure liquid viscosity [9]. For industrial and biomedical applications, the production of porous materials requires the optimization of the density parameter along with mechanical parameters [10]. Here they have used Archimedes' principle to measure the density and area of the given metal form. Mostly density of water is determined using a simple Archimedes' principle. When a known-volume body is submerged in a water sample, the apparent mass loss is equal to the mass of water displaced by the body. The mass of water displaced is the product of the body volume and the density of water at the surrounding temperature [11]. Another simple method to measure the density of a liquid is hydro static pressure sensor methods and, Balanced - columned method [12]–[14].

Optical fiber sensors offer tremendous advantages over existing sensing technologies due to their low weight, high sensitivity, smallness, immune to electromagnetic interference, ease to multiplex many sensors, and robustness for harsh environments [15]. Consales *et al.*, have been proposed the liquid level sensor by using FBG, based on the principle of buoyancy [16]. Sheng *et al.*, developed a temperature-independent high-sensitivity differential pressure sensor based on FBG sensors. Results showed that the sensor is capable of measuring temperature and pressure simultaneously, and it was suitable for the applications of liquid density, specific gravity, liquid level measurement [17]. Chih-Wei Lai *et al.* have been proposed FBG based level sensor with

Manuscript received September 23, 2021; revised November 1, 2021; accepted November 16, 2021. Date of publication November 22, 2021; date of current version December 9, 2021. This work was supported in part by the Indo-Norwegian collaboration in Autonomous Cyber-Physical Systems under Project 287918 of the International Partnerships for Excellent Education, Research and Innovation Program from the Research Council of Norway. *(Corresponding author: Linga Reddy Cenkeramaddi.)*

Venkata Satya Chidambara Swamy Vaddadi, Saidi Reddy Parne, Vijeesh V. P., and Suman Gandi are with the Department of Applied Science, National Institute of Technology Goa, Goa 403401, India (e-mail: swamych@nitgoa.ac.in; psreddy@nitgoa.ac.in; vijeesh@nitgoa.ac.in; gandisuman@nitgoa.ac.in).

Linga Reddy Cenkeramaddi is with the Autonomous and Cyber-Physical Systems Research Group, Department of Information and Communication Technology, University of Agder, 4630 Grimstad, Norway (e-mail: linga.cenkeramaddi@uia.no).

Digital Object Identifier 10.1109/JPHOT.2021.3129587

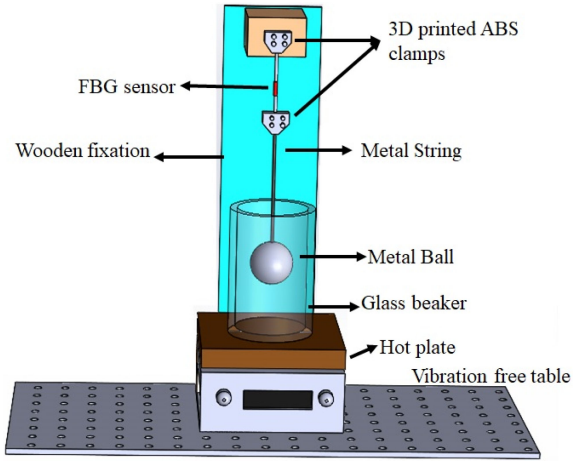

Fig. 1. 3D- Schematic representation of designed sensor.

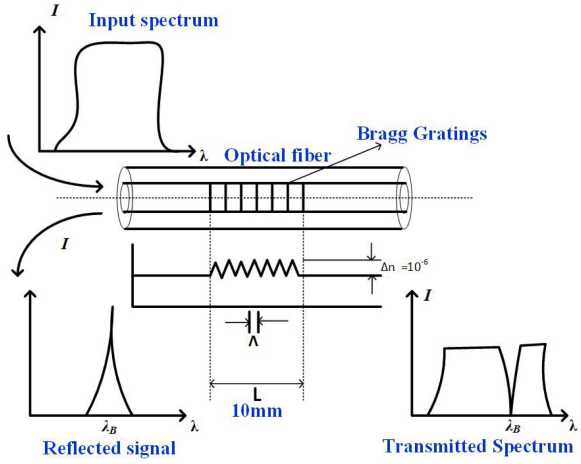

Fig. 2. Schematic representation of FBG operation.

the Fabry Perot pressure sensor combination to measure the liquid level and specific gravity simultaneously [18]. But this sensor has some limitations while measuring specific gravity.

In this study, we demonstrated a method to measure the liquid density with the advantage of low cost, easy fabrication, and high sensitivity based on Archimedes' law of buoyancy. Here we used a fiber Bragg grating (FBG) sensor as a sensing unit. Another FBG sensor is also kept near the previous FBG, which doesn't affect its strain due to liquid density changes. The second FBG is kept to see any temperature effect on the first FBG due to the hot plate. Finally, the sensor's sensitivity is evaluated experimentally, and the analytical formula has been proposed to measure the density of a liquid.

The remainder of this article has been collocated as follows. Section II describes the overview of about FBG sensor, sensor structure, and its implementation with mathematical analysis to find the density of the liquid. Section III describes experimentation with the designed sensor and measurement results of density changes with temperature variation and salt variations in various liquids. Finally, Section IV describes the conclusions and future work.

II. Sensor Design and Implementation

A Schematic representation of the proposed FBG density sensor is shown in Fig. 1. Photo sensitive single mode fiber from Thorlabs was used to inscribe the FBG sensor using the phase mask technique. The physical length of the currently used FBG sensor is 10 mm. We used FBG with a central wavelength of 1550 nm, full width at half maximum (FWHM) 3-db bandwidth of 0.15 nm, and reflectivity of 49.7%. From Fig. 1, it is realized that a metal ball is used as suspending mass and is attached to one end of the fiber, and another end of the fiber is fixed with 3D printed clamps. Since the FBG sensor has no contact with measuring liquid for the measurement, the proposed setup can be used for any liquid. The operating principle of the proposed sensor design relies on Archimedes' law of buoyancy [19]. For this sensor design, we have chosen a simple and low-cost procedure. First, we made a wooden L shape for the fixation of our sensor. This L shape is fixed on the vibration-free table. On top of the L shape, we have attached the 3D printed clamps with screws to hold the fiber. So that fiber is suspended freely in the air. Another 3D printed clamp we fixed at the bottom of the fiber, also these clamps resist the twisting of the fiber, which helps to keep the fiber inline and give proper measurements. From the bottom 3D printed clamp, a metal ball with 82 grams is suspended. So there is an axial strain induced in the FBG sensor, which prompts a wavelength shift in the sensor from the central wavelength.

FBG is an optical device obtained through periodic changing of the refractive index in the core of a single mode fiber [20], [21]. Fig. 2 shows the schematic diagram of the FBG operation principle. It acts as a wavelength-selective filter, such that it reflects a narrow bandwidth and transmits the reaming bandwidth of light [22], [23]. If the reflected waves are in phase, then it will make a constructive interference which causes a strong reflection for a particular wavelength, which is given by Bragg's equation [24], [25].

$$\lambda_B = 2n_{eff}\Lambda \tag{1}$$

Where λ_B is reflected Bragg wavelength, n_{eff} is the effective refractive index of the core, Λ is the pitch of the grating. As a result, when light is launched from the broadband source into the FBG, a light component fulfilled by the above equation will be reflected and lost in the transmitted spectrum. Therefore from the above equation reflected wavelength is strictly depends upon effective refractive index (n_{eff}) and grating pitch (Λ) [26], [27]. FBG sensors have more usages in measuring temperature and strain. An axial strain in the FBG causes to change both n_{eff} and Λ, which results in changing the central wavelength (λ_B) due to the photo elastic and elasto-optic effect, respectively. Similarly, when FBG perturbed with ambient temperature also causes the same effect on gratings due to thermal expansion and thermo-optic effect. When FBG is directly influenced by both temperature and strain at the same time, then the associated wavelength shift is given by [28]–[30],

$$\frac{\Delta\lambda_B}{\lambda_B} = (1 - P_e)\epsilon + (\alpha + \zeta)\Delta T \tag{2}$$

where ϵ is axially applied strain, P_e is photo elastic coefficient of the fiber, α is thermal expansion coefficient, ζ is thermo optic coefficient of the fiber, and ΔT is the temperature variation. From Eq. (2), we are omitting effects due to thermal variations since our FBG sensor measures the density of liquids not having any temperature effect on it. Therefore normalized Bragg wavelength shift due to strain term is

$$\frac{\Delta\lambda_B}{\lambda_B} = (1 - P_e)\epsilon \tag{3}$$

According to Archimedes' law of buoyancy, the total load exerted on the FBG by spherical mass when the ball is dipped in the measuring liquid is combination of both gravitational force and buoyancy force.

$$L_T = Mg - F_A \tag{4}$$

Where L_T is total load exerted on FBG, M is mass of the sphere, g is gravitational acceleration, F_A is buoyancy force of the liquid on mass.

$$\begin{aligned} L_T &= Mg - m_f g \\ &= Mg - d_f V_{mg} \\ &= g(M - d_f V_m) \end{aligned} \tag{5}$$

where m_f is mass of the fluid displaced by the spherical mass is equal to volume of the mass (V_m) is multiplied by density of the fluid (d_f). Mechanical strain applied on the Bragg grating sensor is given by [31]

$$\begin{aligned} \epsilon = \frac{\sigma}{E} &= \frac{L_T}{A \times E} \\ &= \frac{g(M - d_f V_m)}{A \times E} \end{aligned} \tag{6}$$

where σ is axial stress applied on the fiber, A is the areal cross section of the fiber, and E is Young's modulus of the fiber. From 6 it is clearly known that the density of the liquid is directly proportional to axial strain in the fiber. By combining 3 and 6 and by neglecting the temperature effect, normalized wavelength shift is due to variation in liquid density is derived as,

$$\frac{\Delta\lambda_B}{\lambda_B} = (1 - P_e)\frac{g(M - d_f V_m)}{A \times E} \tag{7}$$

From 7 clearly shows that the wavelength shift in FBG depends on the density of the given liquid and the volume of the mass (V_m) suspended in the liquid. In our experiment kept the volume of the mass constant.

$$Sensitivity = \frac{\partial(\Delta\lambda_B)}{\partial d_f} = \frac{-\lambda_B(1 - P_e)gV_m}{A \times E} \tag{8}$$

From the above 8, for a given liquid keeping the level constant, the sensor's sensitivity depends on the radius of the ball, which is suspended in a liquid. Since the volume of the ball is $V_m = \frac{4}{3}\pi r^3$, the sensing performance of the proposed design is suitable for any liquid, and it can be modified according to the required application.

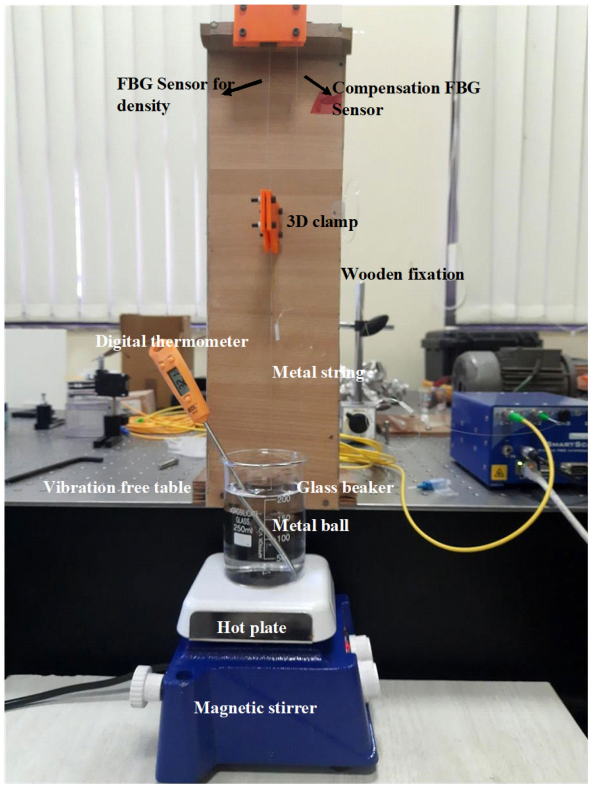

Fig. 3. Experimental setup.

III. Experimental Results and Discussion

The Designed sensor was tested in various liquids to measure the density. First, we have made a wooden fixation on the vibration-free table, and on top of this we fixed a 3D printed clamp to hold the FBG sensor and another end of the FBG freely hanging. To the second end of the FBG, we fixed another 3D printed clamp with a small hole. Due to this, there is a red shift in wavelength, which is considered a central wavelength of FBG. From the second clamp, we hanged a metal ball with a metal wire. This will cause an axial strain in the FBG sensor, and this leads to red shift in wavelength [32]. Fig. 3 shows the experimental setup of the density measurement of liquids. In this experiment, we kept the liquid level constant to restrict the pressure variation, and the liquids used in this experiment have predefined density values. Therefore we can compare measured density values with existing values, which helps us calculate error values in measurements. In all our experiments, we have kept FBG at constant temperature by keeping the room temperature stable with the help of a well maintained air conditioning system. We used an FBG for temperature compensation and observed that there was little or no effect because of the air conditioning system. Observed temperature variation from the compensated FBG wavelength shift is ± 0.7 °C. First, we took 200 ml water with a measuring jar, and we dipped the ball in water so that ball should not touch the bottom of the jar. When we descended the ball in the water, due to buoyancy force acting on the ball, there is stress in the FBG axis which will cause the blue shift in the wavelength, which causes the reduction of the total load (L_T)

TABLE I
DENSITY PARAMETERS

S.No.	Type of liquid	Density (Theory)(kg/m^3)	Density (experimental)(kg/m^3)	error(%)
1.	Water	997.047	913.70	0.0835
2.	Petrol	775	839.06	0.08
3.	Engine oil	872.5	897.60	0.028
4.	Acetone	785.755	863.13	0.09

on the FBG due to buoyant force (F_A). Attention was focused on the fiber tilting and twisting. In the above mentioned way, we have dipped the ball in oil, Petrol, and acetone. We have recorded wavelength shifts for all these liquids several times and taken the average wavelength shifts individually. From the wavelength shift, we calculated density values of the liquid correspondingly, and errors in measurements are tabulated in Table I.

The density of the water is affected due to several reasons. Mainly water is three types: pure water, salt water from oceans, and natural water mostly from lakes. Pure water contains distilled H_2O molecules, including deuterium and tritium molecules. But these heavy water molecules are few and don't show any considerable change in the density of water. Ocean water is composed of several minerals such as Na^+, Cl^-, Mg^+, Ca^+, and SO_4^2-, but mostly Na^+ and Cl^- are having higher proportions compared with remaining minerals, so these proportions definitely affect density function. In lakes, mineral content is constant, and it varies with different lakes, which doesn't produce any change in density. So, in this case the density function varies with the temperature of the water as well as the concentration of salt in it.

A. Temperature Variation

Therefore, we changed the temperature of water from room temperature to 100 °C by varying hot plate temperature with steps of 5 °C variation by keeping salt concentration constant. As the liquids temperature increases, there is greater kinetic energy in the molecules. There are also vibrations in the water molecules, which causes each water molecule to take more space while increasing the temperature. The density of a molecule is represented as mass per unit volume. The density of water decreases with increasing temperature because as temperature rises, the volume of the water molecules increases. The density of pure water varies with temperature by the below equation, and the theoretical graph between temperature with the density of water at 1 atm pressure and s=0 (s= salinity) is plotted in Fig. 4 [33].

$$\rho = \left\{ \left[1 - \frac{(T - 3.9863)^2}{508929.2} \frac{T + 288.9414}{T + 68.12963} \right] \times 0.99973 \right\} \times P_L \times A_L \tag{9}$$

where

$$P_L = \frac{1}{1 - c(p-1)}$$

$$A_L = 1 - (2.11 - 0.053\,T) \times \left(1 - \frac{1}{1+t}\right) \times 10^{-6}$$

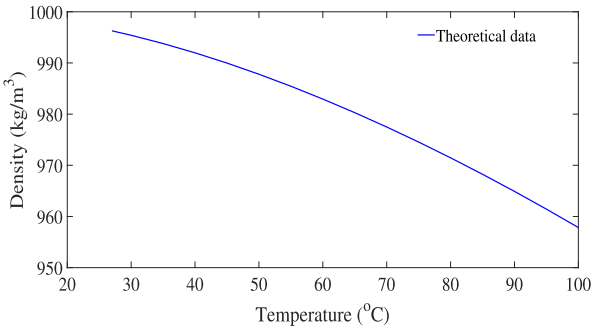

Fig. 4. Theoretical curve between temperature and density.

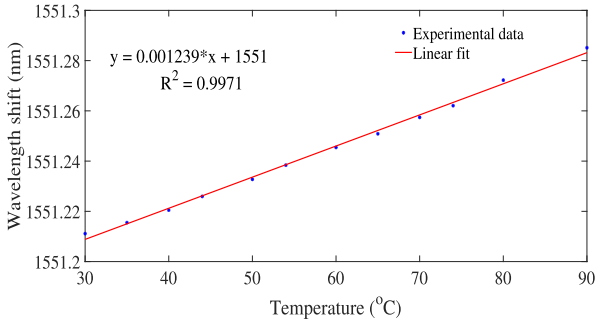

Fig. 5. Experimental curve between temperature of liquid and wavelength shift.

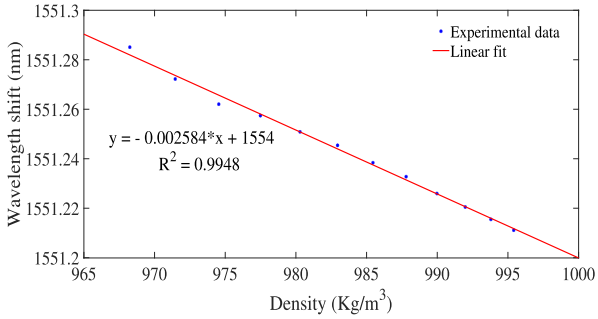

Fig. 6. Experimental curve between liquid density versus wavelength shift.

Where T is temperature measured in degree Celsius, p is atmospheric pressure, c is a measure of compressbility, and t is the time measured in terms of days. Since we have done the whole experiment at 1 atm pressure, therefore $P_L = 1$.

Wavelength shift with temperature variation is plotted in Fig. 5, since an increase in the temperature of liquid causes the change in density of the liquid. Due to the change in density of the liquid, the buoyancy force acting on the ball gets reduces, which causes more strain in the FBG. Therefore, while increasing the temperature of the liquid, the wavelength shift in the FBG also increases.

The temperature of the liquid is increased initially to 30 C and then gradually raised upto 100 °C with 5 °C increments using the help of hot plate and digital thermometer readings. We have calculated the density of liquid water by using 9. The graph between calculated density versus wavelength shift in the FBG is plotted in Fig. 6. From both Figs. 5 and 6, it is clearly noted

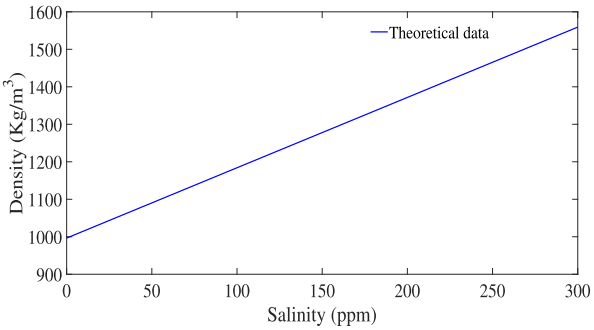

Fig. 7. Theoretical curve of liquid density variation with salinity of liquid.

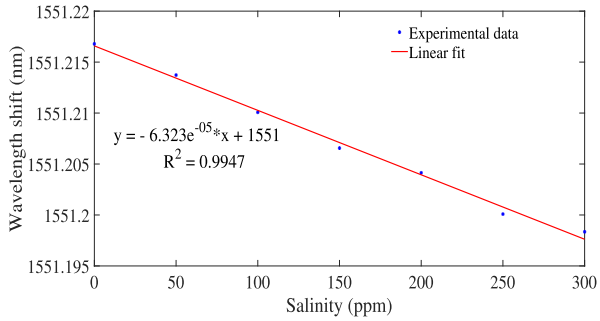

Fig. 8. Experimental curve between salinity of liquid versus wavelength shift.

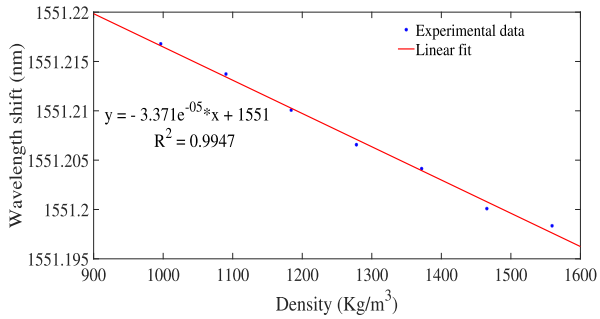

Fig. 9. Experimental curve between density of liquid versus wavelength shift.

that FBG wavelength shift varies linearly with the density of liquid varied by temperature. The measured density sensitivity of the sensor is 2.584 pm/Kg/m^3 with an excellent linearity coefficient ($R^2 = 0.9948$). Therefore, our proposed sensor design can measure the density changes due to temperature variation in liquid.

B. Salinity Variation

Natural water and seawater are distinguished from pure water by the addition of different kinds of salts. Out of all salts, $NaCl$ percentage is more in see water, the density function of seawater affected by this salt concentration. The below equation calculates density function varied with salinity [34].

$$\rho(T, S) = \rho_1(T) + \rho_2(T)S \tag{10}$$

where

$$\rho_1(T) = 999.8395 + 6.7914 \times 10^{-2}T - 9.0894 \times 10^{-3}T^2 + 1.0171 \times 10^{-4}T^3 - 1.2846 \times 10^{-6}T^4 + 1.1592 \times 10^{-8}T^5 - 5.0125 \times 10^{-11}T^6$$

$$\rho_2(T) = 8.181 \times 10^{-1} - 3.85 \times 10^{-3}T + 4.96 \times 10^{-5}T^2$$

Where ρ denotes the density of water, which varies with temperature and salinity, T is the temperature in degrees Celsius, and S denotes the salinity in grams of salt added per kilogram of pure water. If S = 0, then this equation will get the same results as 9. In Fig. 7, a theoretical graph is presented between the density of water altered by the addition of salt and it clearly shows a linear relationship between them at room temperature (27 °C).

The density of the liquid is measured experimentally with the help of the FBG sensor by varying salinity, different concentrations of salt from 0 to 300 ppm is added to the 400 ml of water in a beaker, which is placed on a magnetic stirrer with a small pallet to mix the added salt properly. Since a metal ball is used to measure the density of the liquid, Between metal ball and pallet, there is a magnetic attraction force that causes an extra shift in wavelength, which causes error in values. Therefore before every measurement, the pallet is removed from the beaker. By adding salt to the liquid, the buoyancy force acting on the ball will increase. Therefore total strain acting on the FBG gradually decreases with salt, which results in the decrease in wavelength shift for each ppm of salt. Fig. 8 represents the wavelength shift in FBG with salinity variation in the liquid. Since the density function is affected by added salt, we calculated the density variations in water for each ppm of salt by using 10. The graph between calculated density and corresponding wavelength shift in the FBG is plotted in Fig. 9. This shows the wavelength shift varies linearly with density variation due to salt concentration. From the slope of the graph, sensitivity of the sensor to density is determined as 3.375×10^{-2} pm/Kg/m^3 with linearity coefficient $R^2 = 0.9947$. From Figs. 8 and 9 it is noted that the FBG sensor is capable of measuring the change in density of liquid due to salt concentration variation at a constant temperature.

In the previous two sections, we measured liquid density by varying temperature at constant salinity, and by varying salinity at a constant temperature. In both cases, our proposed sensor design showed good results. Now we changed both temperature and salinity of liquid simultaneously to measure density variations. First, we took 800 ml of water in the beaker and varied the temperature constantly from room temperature to 100 °C with zero salinity. Second, we added 50 ppm of salt to the water and heated it again to 100 °C, and the experimentation is repeated for 100 ppm, 200 ppm, 300 ppm. Results are plotted in Fig. 10. From previous discussions, density is directly proportional to salinity and inversely proportional to temperature. Therefore, wavelength shift decreases with increasing the salinity concentration and increases with temperature. With this analogy and from the Fig. 10 it is seen that at low ppm of salt and at high-temperature wavelength shift is more compared with higher ppm of salt. Different salt concentrations mostly dominate a change in the density of a liquid compared with temperature variations.

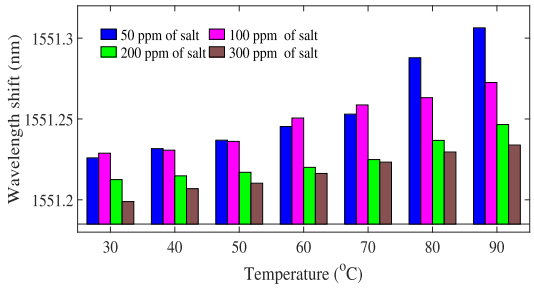

Fig. 10. Temperature of liquid versus Density.

IV. Conclusion

We proposed the design, implementation, and experimental demonstration of the optical density sensor based on the FBG strain sensor for liquid density measurement. The proposed sensor principle relies on Archimedes' law of buoyancy and the total strain reduced in FBG due to the load exerted by the suspended mass. In our experiments demonstrated the proposed sensor for the density measurement of water, petrol, engine oil, and acetone. We also calculated the density errors with predefined density values of those liquids. In the sensor design, we used a metal ball as a suspended mass in the liquid, with a radius of 13.5 mm and 82 grams. By changing the geometrical parameters of the ball, the sensitivity of the sensor can be tailored. To change the density of a liquid, we varied its temperature from room temperature to 100 °C, and its salinity varied from 0 ppm to 300 ppm. In above, both cases sensitivity of the sensor is determined as $2.584\,\mathrm{pm/Kg/m^3}$ and $3.375 \times 10^{-2}\,\mathrm{pm/Kg/m^3}$ respectively. We've also studied the density of liquid when both salinity and temperature are varied at the same time. In the future, by modifying the setup in such a way that by introduce an appropriate spring system, we can use this setup as a vibration measurement sensor for under water autonomous vehicles. If this system required to work on the surface of earth, there must be some kind of compensation techniques to overcome the seismic events and vibrations around the globe. The system works as a basic spring and mass system for vibration measurements.

References

[1] M. Khorsandi and S. Feghhi, "Design and construction of a prototype gamma-ray densitometer for petroleum products monitoring applications," *Measurement*, vol. 44, no. 9, pp. 1512–1515, 2011.

[2] C.-H. Tsai and W. Lick, "A portable device for measuring sediment resuspension," *J. Great Lakes Res.*, vol. 12, no. 4, pp. 314–321, 1986.

[3] S. Rizzolo *et al.*, "Real time monitoring of water level and temperature in storage fuel pools through optical fibre sensors," *Sci. Rep.*, vol. 7, no. 1, pp. 1–10, 2017.

[4] T. Guo *et al.*, "Temperature-insensitive fiber Bragg grating liquid-level sensor based on bending cantilever beam," *IEEE Photon. Technol. Lett.*, vol. 17, no. 11, pp. 2400–2402, Nov. 2005.

[5] K.-R. Sohn and J.-H. Shim, "Liquid-level monitoring sensor systems using fiber Bragg grating embedded in cantilever," *Sensors Actuators A: Phys.*, vol. 152, no. 2, pp. 248–251, 2009.

[6] B. Preložnik, D. Gleich, and D. Donlagic, "All-fiber, thermo-optic liquid level sensor," *Opt. Exp.*, vol. 26, no. 18, pp. 23 518–23 533, 2018.

[7] F. Pradelle, S. L. Braga, A. R. F. Martins, F. Turkovics, and R. N. Pradelle, "Gum formation in gasoline and its blends: A review," *Energy Fuels*, vol. 29, no. 12, pp. 7753–7770, 2015.

[8] K. Loizou and E. Koutroulis, "Water level sensing: State of the art review and performance evaluation of a low-cost measurement system," *Measurement*, vol. 89, pp. 204–214, 2016.

[9] Y. Sato, H. Yoshioka, S. Aikawa, and R. L. Smith, "A digital variable-angle rolling-ball viscometer for measurement of viscosity, density, and bubble-point pressure of CO_2 and organic liquid mixtures," *Int. J. Thermophysics*, vol. 31, no. 10, pp. 1896–1903, 2010.

[10] D. Fulginiti, S. Grassini, E. Angelini, and M. Parvis, "Indirect material density measurement by a simple digital imaging method," in *Proc. IEEE Int. Instrum. Meas. Technol. Conf. Proc.*, 2016, pp. 1–6.

[11] S. Gupta, *Practical Density Measurement and Hydrometry*. Boca Raton, FL, USA: CRC Press, 2002.

[12] A. Puttmer, P. Hauptmann, and B. Henning, "Ultrasonic density sensor for liquids," *IEEE Trans. Ultrasonics, Ferroelectrics, Freq. Control*, vol. 47, no. 1, pp. 85–92, Jan. 2000.

[13] F. Spieweck and H. Bettin, "Solid and liquid density determination," *Tm-Technisches Messen*, vol. 59, no. 7-8, pp. 285–292, 1992.

[14] F. Spieweck, "Sensors for measuring density and viscosity," *Sensors: Mech. Sensors*, vol. 7, pp. 359–372, 1993.

[15] R. Kashyap, *Fiber Bragg Gratings*. Cambridge, MA, USA: Academic Press, 2009.

[16] M. Consales *et al.*, "A fiber Bragg grating liquid level sensor based on the Archimedes' law of buoyancy," *J. Lightw. Technol.*, vol. 36, no. 20, pp. 4936–4941, Aug. 2018.

[17] H.-J. Sheng, W.-F. Liu, K.-R. Lin, S.-S. Bor, and M.-Y. Fu, "High-sensitivity temperature-independent differential pressure sensor using fiber Bragg gratings," *Opt. Exp.*, vol. 16, no. 20, pp. 16013–16018, 2008.

[18] C.-W. Lai, Y.-L. Lo, J.-P. Yur, and C.-H. Chuang, "Application of fiber Bragg grating level sensor and Fabry-Perot pressure sensor to simultaneous measurement of liquid level and specific gravity," *IEEE Sensors J.*, vol. 12, no. 4, pp. 827–831, Apr. 2012.

[19] H. Keighley, "Archimedes' Principle and Flotation," in *Work Out Physics 'o'level and GCSE*. Berlin, Germany: Springer, 1986, pp. 58–64.

[20] Y.-J. Rao, "Recent progress in applications of in-fibre Bragg grating sensors," *Opt. Lasers Eng.*, vol. 31, no. 4, pp. 297–324, 1999.

[21] C. E. Campanella, A. Cuccovillo, C. Campanella, A. Yurt, and V. Passaro, "Fibre Bragg grating based strain sensors: Review of technology and applications," *Sensors*, vol. 18, no. 9, 2018, Art. no. 3115.

[22] V. S. C. S. Vaddadi, S. R. Parne, S. Afzulpurkar, S. P. Desai, and V. V. Parambil, "Design and development of pressure sensor based on fiber Bragg grating (FBG) for ocean applications," *Eur. Phys. J. Appl. Phys.*, vol. 90, no. 3, 2020, Art. no. 30501.

[23] D. Sengupta, M. Sai Shankar, P. Saidi Reddy, R. Sai Prasad, and K. Srimannarayana, "Sensing of hydrostatic pressure using FBG sensor for liquid level measurement," *Micro. Opt. Technol. Lett.*, vol. 54, no. 7, pp. 1679–1683, 2012.

[24] V. Mishra *et al.*, "Fiber Bragg grating sensor for monitoring bone decalcification," *Orthopaedics Traumatol.: Surg. Res.*, vol. 96, no. 6, pp. 646–651, 2010.

[25] D. Sengupta *et al.*, "Axial strain based Bragg grating level sensor," *Optoelectron. Adv. Mater.-Rapid Commun.*, vol. 4, pp. 1933–1936, 2010.

[26] K. O. Hill and G. Meltz, "Fiber Bragg grating technology fundamentals and overview," *J. Lightw. Technol.*, vol. 15, no. 8, pp. 1263–1276, Aug. 1997.

[27] A. Othonos, "Fiber Bragg gratings," *Rev. Sci. Instrum.*, vol. 68, no. 12, pp. 4309–4341, 1997.

[28] P. S. Reddy *et al.*, "Method for enhancing and controlling temperature sensitivity of fiber Bragg grating sensor based on two bimetallic strips," *IEEE Photon. J.*, vol. 4, no. 3, Jun. 2012.

[29] C. Wu, Y. Zhang, and B.-O. Guan, "Simultaneous measurement of temperature and hydrostatic pressure using bragg gratings in standard and grapefruit microstructured fibers," *IEEE Sensors J.*, vol. 11, no. 2, pp. 489–492, Feb. 2011.

[30] L. Xue *et al.*, "Method for enhancing temperature sensitivity of fiber Bragg gratings based on bimetallic sheets," *Appl. Opt.*, vol. 45, no. 31, pp. 8132–8135, 2006.

[31] B. R. Munson, T. H. Okiishi, W. W. Huebsch, and A. P. Rothmayer, *Fluid Mechanics*. Hoboken, NJ, USA: Wiley, 2013.

[32] W. Zhang, X. Dong, Q. Zhao, G. Kai, and S. Yuan, "FBG-type sensor for simultaneous measurement of force (or displacement) and temperature based on bilateral cantilever beam," *IEEE Photon. Technol. Lett.*, vol. 13, no. 12, pp. 1340–1342, Dec. 2001.

[33] K. Hutter, Y. Wang, and I. P. Chubarenko, "Phenomenological coefficients of water," in *Physics of Lakes*. Berlin, Germany: Springer, 2011, pp. 389–418.

[34] D. Jamieson, J. Tudhope, R. Morris, and G. Cartwright, "Physical properties of sea water solutions: Heat capacity," *Desalination*, vol. 7, no. 1, pp. 23–30, 1969.